Driving Forces for Adsorption of Amphiphilic Peptides to the Air−Water Interface

ARTICLE *in* THE JOURNAL OF PHYSICAL CHEMISTRY B · SEPTEMBER 2010

Impact Factor: 3.3 · DOI: 10.1021/jp1024922 · Source: PubMed

4 AUTHORS, INCLUDING:

Ozge Sensoy
Weill Cornell Medical College
12 PUBLICATIONS **67** CITATIONS
SEE PROFILE

Mehmet Sayar
Koc University
36 PUBLICATIONS **328** CITATIONS
SEE PROFILE

Driving Forces for Adsorption of Amphiphilic Peptides to the Air−Water Interface

Ozge Engin,[†] Alessandra Villa,[‡,§] Mehmet Sayar,[†] and Berk Hess*[,‡,||]

College of Engineering, Koc University, Istanbul, Turkey, Max-Planck Institute for Polymer Research, D-55128, Mainz, Germany, Karolinska Institutet, SE-14157, Huddinge, Sweden, Stockholm Center for Biomembrane Research, Stockholm University, SE-10691 Stockholm, Sweden, and Center of Smart Interfaces, Technical University of Darmstadt, D-64287 Darmstadt, Germany

Received: March 19, 2010; Revised Manuscript Received: June 28, 2010

We have studied the partitioning of amphiphilic peptides at the air−water interface. The free energy of adsorption from bulk to interface was calculated by determining the potential of mean force via atomistic molecular dynamics simulations. To this end a method is introduced to restrain or constrain the center of mass of a group of molecules in a periodic system. The model amphiphilic peptides are composed of alternating valine and asparagine residues. The decomposition of the free energy difference between the bulk and interface is studied for different peptide block lengths. Our analysis revealed that for short amphiphilic peptides the surface driving force dominantly stems from the dehydration of hydrophobic side chains. The only opposing force is associated with the loss of orientational freedom of the peptide at the interface. For the peptides studied, the free energy difference scales linearly with the size of the molecule, since the peptides mainly adopt extended conformations both in bulk and at the interface. The free energy difference depends strongly on the water model, which can be rationalized through the hydration thermodynamics of hydrophobic solutes. Finally, we measured the reduction of the surface tension associated with complete coverage of the interface with peptides.

I. Introduction

Understanding the structure and organization of amphiphilic molecules at the air−water interface is of interest for various research fields, from materials science to biology. The air−water interface provides a well-defined two-dimensional environment to study and control molecular self-assembly. The evolving field of molecular self-assembly aims at designing and controlling the shape of molecular clusters by controlling intermolecular interactions. Such well controlled clusters might find many application areas in material science such as thin-layered microstructures.[1] On the other hand, the air−water interface may also be used to mimic hydrophobic/hydrophilic interface of cellular membranes. This simplifies the study of protein-like systems that are surface active and/or self-assemble within membranes.[2−4]

Among amphiphilic molecules, poly peptides have been widely studied both as protein analogs and as building blocks for new types of biomaterials. These peptides are characterized by alternating hydrophobic and hydrophilic side chains. Amphiphilic peptides can form ordered structures at interfaces using secondary structural elements of proteins (such as β-strands, helices, and turns).[5,6] Such an ordered monolayer provides planar scaffolds relevant to a broad spectrum of applications from photoactive films to cell guidance substrates. Interestingly, amphiphilic peptides occur also in nature among antimicrobial molecules[7] whose proposed mechanisms of action involve interaction with the cellular membrane. To improve the design of new peptide-based systems, for medical and technological applications, it is important to understand the role of the amino-acid sequence (type, length, etc.) in adsorption processes.

Experimentally, these systems can be studied at interfaces by Langmuir techniques, spectroscopic measurements, and atomic force microscopy.[8−10] Nevertheless, these techniques cannot provide direct information on the molecular conformation at the interface or on the specific thermodynamic contributions to the adsorption free energy. An alternative to study processes at the surface is molecular simulation. Note that in simulations the air−water interface is replaced by a water liquid−vapor interface, which is a reasonable approximation, since there are very few molecules in the air or vapor. Atomistic simulations have been widely used to understand in detail the adsorption process of small molecules to the air−water interface (a detailed review has recently been published by Garrett et al.[11]). Adsorption free energies at the air−water interface have also been estimated for peptide systems using computer simulations with an empirical force field. Gu et al.[12] combined Monte Carlo sampling with an implicit solvent model to calculate adsorption free energy of a set of designed surface active peptides. Miller et al.[3] studied the adsorption of amphiphilic β-peptides at the air−water interface using molecular dynamic simulations and explicit solvent description. To obtain the free energy, they calculated the potential of mean force (PMF) for the peptides between the bulk and interface using a set of distance constraint independent 2 ns simulations.

Here, we use extensive molecular dynamics simulations to give a detailed picture of the adsorption of amphiphilic peptides to the air−water interface. In particular, we aim to analyze different contributions to the free energy difference and understand if there is a correlation between peptide length and the driving force for adsorption. To this end we chose model peptides with an alternating sequence of hydrophobic valine and hydrophilic asparagine residues. The simulated peptides are capped and differ in the number of Val-Asn blocks: Ace-(Val-Asn)-NME where blocks of $n = 1$, 2, 3, and 5 were used, which

[†] Koc University.
[‡] Max-Planck Institute for Polymer Research.
[§] Karolinska Institutet.
[||] Stockholm University and Technical University of Darmstadt.

10.1021/jp1024922
Published on Web 08/05/2010

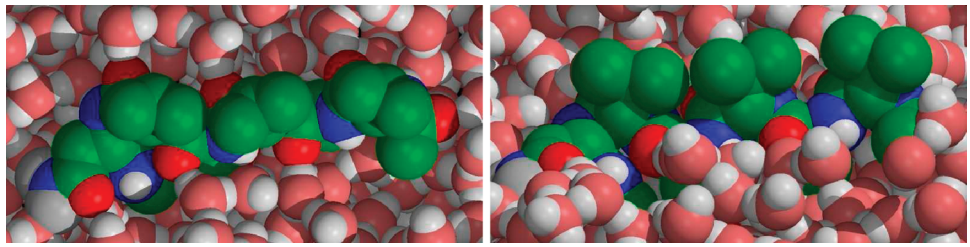

Figure 1. Top and side view of a typical conformation of the hexapeptide at the interface with SPC/E water. The alternating sequence of hydophobic and hydrophilic residues enables robust partitioning of the molecule at the interface, with all three valine side chains sticking into the air.

TABLE 1: Hydration Thermodynamic Properties of the Analogues of the Amino Acid Side Chains of Valine and Asparagine at 298 K in kJ/mol

	propane			acetamide		
force field	ΔG	ΔH	$T\Delta S$	ΔG	ΔH	$T\Delta S$
G53A6 + SPC[16]	7.8	−10.5	−18.3	−43.1	−66.9	−23.8
G53A6 + SPC/E[16]	8.9	−13.8	−22.7	−42.3	−67.2	−24.9
precision	0.2	0.8	0.8	0.3	0.8	0.8
experiment[17,18]	8.3	−13.7	−22.0	−40.5	−67.0	−26.5

we refer to as di-, tetra-, hexa-, and decapeptide in the manuscript, respectively. Figure 1 shows an example of the hexapeptide at the air−water interface. We have used two water models, which serves two purposes: it shows that choosing a good water model is important, but it also gives insight in to the different contributions to the free energy.

We will first show accurate free energy profiles for single peptides as a function of the distance from the interface. To measure the force acting on a peptide at a given distance from the interface, we introduce a method for constraining molecules in a periodic system. For the dipeptide we also determined the enthalpy, such that enthalpic and entropic contributions can be distinguished. We will compare the free energy differences obtained from changing the distance to those from changing one water model into another using Bennett's acceptance ratio method. And, finally, we show the structure of an interface completely covered with peptides and the effect on the surface tension.

II. Methods

One of the most important choices that has to be made for simulations in general, and especially for simulating partitioning of molecules between different environments, is the force field. Hydration free energy of hydrophobic side chains is one of the main driving forces to push the amphiphilic peptides to the air−water interface. Therefore, we chose the GROMOS G53A6 force field, which has been parametrized to reproduce the hydration free energies of amino acid analogs.[13] For the water molecules two different models are used: SPC[14] and SPC/E.[15] The former has been used for the parametrization of the GROMOS G53A6 force field and the latter has been shown to provide accurate hydration free energies.[16]

Hydration free energy and its partitioning into enthalpic and entropic contributions for the analogues of the amino acid side chains of the two residues present in the model peptide are available in the literature.[16] Results for both SPC and SPC/E water models, and the experimental data (for comparison) are given in Table 1. The calculated hydration free energy for propane is fairly good, while for acetamide it is slightly underestimated. It is seen that the composition of the free energy is strongly affected by the water model. SPC overestimates the hydration enthalpy and entropy of propane, whereas both water models slightly overestimate the hydration entropy of acetamide. The hydration enthalpy and entropy have large, compensating solvent contributions. SPC/E does better for both propane and acetamide mainly because it better reproduces hydration of hydrophobic solutes. In SPC/E the more unfavorable hydration of the methyl group is compensated by stronger hydrogen bonds between acetamide and water. We expect that the chosen force field will perform well at 298 K. We do not have data for an analogue of the backbone, but since the backbone and the force field for it are quite similar to those of acetamide, this should also have good partitioning properties. The capped end groups are composed of building blocks similar to the ones considered so far; therefore, we expect a similar level of accuracy.

All simulations were performed with the Gromacs 4.0 molecular simulation package.[19] The particle mesh Ewald (PME) method[20] was used for the electrostatics with a real space cutoff of 1.0 nm and a grid spacing of 0.13 nm. The Lennard-Jones (LJ) interactions were determined with a twin-range cutoff scheme of 1.0 and 1.4 nm with the long-range interactions updated every 10 steps. The time step was 2 fs. The temperature was coupled to 298 K using the Berendsen thermostat.[21] Bond lengths were constrained using SETTLE[22] for the water and P-LINCS for the peptide.[23]

For bulk simulations the peptides were solvated in cubic unit cells ranging from 3.1 nm (1000 H_2O) for the dipeptide to 5.8 nm for the decapeptide (6336 H_2O). For the interface simulations the height of the box was increased by a factor of 3 to create a vacuum of twice the size of the water slab. A slab correction was applied for PME.[24] In the PMF simulations the distance in the z-dimension between the centers of mass of the water slab and the peptide was constrained. PMF calculations were also performed for acetamide.

A common problem that can occur with this setup is that water molecules can escape from the bulk water phase and enter the vapor phase. Once this happens a molecule will travel at (near) constant speed and will join the bulk water phase on the other side through the periodic boundary in the z-direction. If the center of mass of the water molecules is simply determined as the center of mass within the unit cell, the jump of a molecule over the periodic boundary will result in discontinuities in the constraint force. Apart from introducing a small error in the integration of the equations of motion, this also complicates the analysis. These events become more common as simulation time and size increases. One can ignore (part of) the problem by filtering out the spikes in the constraint force, but we decided to resolve this issue by designing a constraining procedure that takes periodicity properly into account, which is described in the Appendix.

For obtaining the PMF curves, the data points were sampled with 0.1 nm spacing. The mean force was accumulated over 20 ns for acetamide and the di- and tetrapeptides and over 40−80 ns for the hexapeptide. Additional simulations of 50−160 ns were performed in bulk water and of 500−1750 ns at the

interface to determine the bulk and interface properties. Interface properties were determined from additional unconstrained interface simulations or from the constrained simulations through Boltzmann averaging with the PMF values. Standard error estimates were determined using block averaging taking into account possible long time correlations.[25]

III. Results and Discussion

A. Water Surface Tension. Since reduction of the surface tension of water is one of the main forces driving amphiphiles to an interface, we calculated the surface tension of SPC and SPC/E under the conditions used for the peptide simulations. The combined tension γ of both air−water interfaces is given by the difference of the normal and lateral pressure multiplied by the height of the unit cell l_z:

$$2\gamma = \left[P_{zz} - \frac{1}{2}(P_{xx} + P_{yy})\right] l_z \qquad (1)$$

To this end we performed simulations of a slab of 1728 water molecules (3.7 nm in each dimension) for 500 ns to determine the surface tension of the air−water interface. The surface tension was determined as 52.2 ± 0.05 mJ/m^2 for SPC and 59.5 ± 0.05 mJ/m^2 for SPC/E. The experimental value at 298 K is 72 mJ/m^2.[26] An analytical correction for the dispersion interactions beyond the cutoff distance can be made, assuming a flat surface and a uniform dispersion density within the slab. The correction for both water models beyond the cutoff distance of 1.4 nm is 1.9 mJ/m^2. For a peptide at the interface the correction might change slightly, because the interface may deform to some extent close to the peptide. In water the dispersion correction is small relative to the long-range electrostatic forces; for a thorough analysis, see, for instance, ref 27. Since the PMF simulations were performed with the Berendsen thermostat, we used the same thermostat for comparing the surface tensions of pure water. We additionally performed 500 ns simulations with the velocity-rescale thermostat,[28] which, unlike the Berendsen thermostat, guarantees a canonical ensemble, and the surface tension for both water models is 0.1 mJ/m^2 higher. This difference is very small, but just above the statistical accuracy.

Both water models significantly underestimate the surface tension, with the error for SPC being twice as large as for SPC/E. The absence of dispersion interactions beyond the interface accounts for part of the discrepancy between experimental and computed values. This term will not change when a peptide is transferred to the interface, because the dispersion density of peptides is equal to that of water. It is difficult to quantify this term, since in water the effect of different potential terms cannot be separated easily. From the calculated surface tension values, we expect that the free energy difference for transferring an amphiphilic peptide from bulk to the air−water interface will be significantly larger with SPC/E than with SPC. However, simulations with both water models probably still underestimate the free-energy differences compared to the real value.

B. Potentials of Mean Force. The PMF curves for the di-, tetra-, and hexapeptides in SPC and SPC/E water are shown in Figures 2 and 3, respectively. The decapeptide switches between extended and collapsed conformations on a time scale of tens of nanoseconds in bulk. When (partially) at the interface, these transitions are further slowed down. Since these two states show quite a different mean force, obtaining a converged PMF turned out to be computationally too expensive for the decapeptide. The origin along the z-axis was chosen as the location of the water interface, which we defined as the point where the water

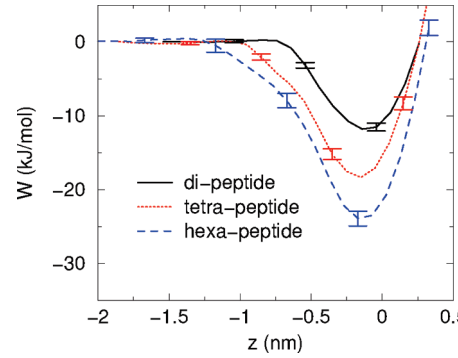

Figure 2. PMF of the di-, tetra-, and hexapeptide in SPC water as a function of the distance from the center of mass of the peptide to the interface. Note that points are spaced by 0.1 nm, while error estimates are only plotted every 0.4 nm.

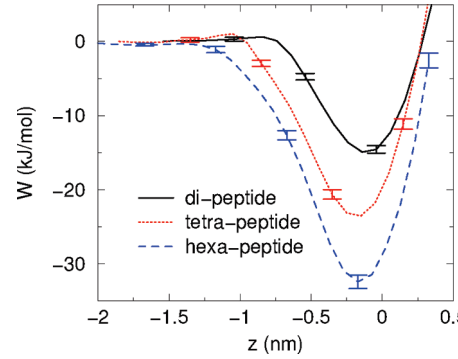

Figure 3. As Figure 2, but in SPC/E.

density is at half the bulk density. Note that for both water models the minima in PMF curves are slightly below the interface, which is consistent with the fact that a larger portion of the peptides is hydrophilic. This can also be confirmed with the snapshot for hexapeptide shown in Figure 1, which represents a typical conformation of the peptide at the PMF minimum.

Although all our interface simulations were performed in a constant-NVT ensemble, we will still refer to the free energy as G and to enthalpy instead of energy, since experiments are usually performed at constant pressure and the volume changes are so small that the $p\Delta V$ term is always smaller than the statistical accuracy of the simulations. Defining a free energy for partitioning between the bulk and the interface is not straightforward, since it will depend on the amount of bulk that is present below the interface. To obtain a definition that does not require a reference length scale of the bulk, the free energy for constraining a particle is required. This involves the mass of the molecule and Dirac's constant (see, e.g., ref 11 for details). The dependence on mass is inconvenient for interpreting the change in ΔG values for different peptide lengths, because the mass does not play a role in the thermodynamics of partitioning. We therefore decided to determine the free energy with respect to a reference thickness of the bulk layer l:

$$\Delta G^l = -k_B T \log\left[\frac{1}{l}\int_{\text{well}} \exp\left(-\frac{W(z)}{k_B T}\right) \mathrm{d}z\right] \qquad (2)$$

where W is the PMF with a reference value of 0 in the bulk. The integral is performed over the well at the interface. The precise extent of the well is not critical; since the minimum is several $k_B T$ deep, varying the boundaries has a negligible effect.

TABLE 2: Ensemble Average of the Work ($\langle W \rangle$) and the Free Energy for Moving a Peptide and Acetamide from Bulk Water to the Air−Water Interface (ΔG^{1nm}) in kJ/mol

	molecule	$\langle W \rangle$	ΔG^{1nm}
SPC	acetamide	-3.9 ± 0.2	-2.0 ± 0.2
	dipeptide	-11.0 ± 0.5	-9.1 ± 0.5
	tetrapeptide	-17.4 ± 0.8	-15.2 ± 0.8
	hexapeptide	-23.1 ± 1.0	-20.7 ± 1.0
SPC/E	acetamide	-4.9 ± 0.2	-2.9 ± 0.2
	dipeptide	-14.1 ± 0.5	-12.1 ± 0.5
	tetrapeptide	-22.8 ± 0.7	-20.4 ± 0.7
	hexapeptide	-31.6 ± 0.9	-29.0 ± 0.9

The free energy difference can be easily transformed to another reference length h by adding a term $-k_BT \log l/h$. The dependence on a reference bulk layer thickness drops out since we are interested in the change in ΔG between different peptides.

In Table 2 we report ΔG^l obtained from the integration of PMF curves in Figures 2 and 3 based on a reference length of 1 nm. This length corresponds to 4 times the average width of the distribution at the interface (0.25 nm) measured as 2 times the standard deviation. The first thing to notice is that the free energy depends linearly on the peptide length when going from 2 to 6 residues, in both SPC and SPC/E. One can see that the free-energy difference between bulk and interface is around 30% larger for SPC/E than for SPC. As stated above, this is expected on the basis of the surface tension of the water models. The effect can also been seen in the hydration free energies of the small molecules in Table 1. We will analyze this in more detail later.

Another useful quantity is the ensemble averaged work $\langle W \rangle$ for transferring a peptide to the interface. It can be computed as W averaged over the interface region with the Boltzmann factor of W:

$$\langle W \rangle = \int_{\text{well}} W(z) \exp\left(-\frac{W(z)}{k_BT}\right) dz \qquad (3)$$

This measures the free energy difference for inserting a peptide in the bulk and at the interface; it is ΔG without the entropic contribution of the center of mass of the peptide. This quantity is useful for interpreting different contributions to ΔG, because it measures only the contributions due to differences in environment (note that this still includes changes in peptide conformational states). Unlike ΔG, it does not depend on the amount of bulk below the interface. Results for $\langle W \rangle$ are also reported in Table 2. The difference between $\langle W \rangle$ and ΔG^{1nm} is 2.2 kJ/mol on average and are within error margins, which shows that the entropy loss of the center of mass of the peptide at the interface is the same for all cases.

To determine the enthalpic and entropic contributions to the free energy, we also performed simulations of 40 ns for the dipeptide in SPC/E and measured the average potential energy. Subtracting the enthalpy from the PMF can give the entropic contribution. The results are shown in Figure 4, where the PMF is denoted by W. As the peptide moves from bulk to the interface, there is a minimum in the enthalpy at −0.4 nm. The entropy does not show a significant change at this distance. Here most of the time the peptide is completely in the solvent, except for the side chain of valine (see Figure 1). The enthalpy change of 12 kJ/mol is close to what one would expect on the basis of the value for propane in Table 1. The entropy change, however,

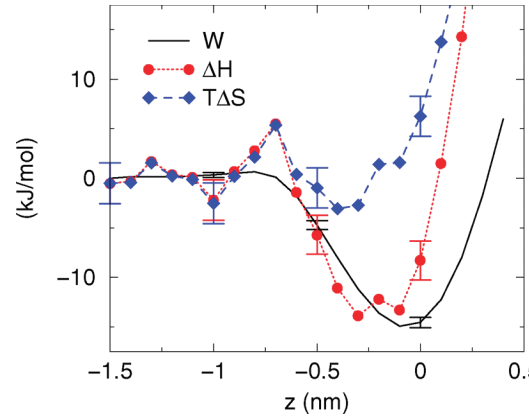

Figure 4. PMF, enthalpy, and entropy differences for the dipeptide in SPC/E as a function of distance to the interface.

is negligible and cannot be explained as a simple desolvation of the side chain of valine. Apparently, the entropy gain of the water molecules that lose contact with the hydrophobic side chains is compensated by, among other things, an entropy loss of conformational degrees of freedom of the peptide. As the peptide moves further beyond the interface, both ΔH and ΔS increase, as one would expect from the solvation properties of the propane and acetamide moieties. Eventually, one would expect that these contributions converge to the values of a dipeptide in vacuum. However, even at the largest distance analyzed here, there is still a water meniscus that bridges the peptide to the bulk water, and therefore we do not observe such a behavior.

In the following section we will analyze different contributions to the free energy change.

C. Decomposition of the Free Energy. The free energy of transferring an amphiphilic molecule from bulk water to the air−water interface can be decomposed into three main contributions. Two contributions can be attributed to the solvent, although they are caused by changes in the interface between peptide and water: the desolvation of hydrophobic groups and the decrease of the air−water interface area. A third contribution can be attributed to the peptide, although it is caused by changes in the solvent environment: entropy changes due to changing weights of peptide conformational states. This can in turn be decomposed into internal and center of mass degrees of freedom.

We will start with the first contribution. The backbone and the asparagine side chains are similar to those of acetamide, with one or more hydrogens replaced by other moieties. The asparagine side chains remain solvated during all the simulations, and we therefore do not expect that they contribute significantly to the free energy difference. But the backbone is partially dehydrated at the interface. The $\langle W \rangle$ value for acetamide is 1 kJ/mol lower in SPC/E than in SPC (Table 2), which is exactly opposite to the hydration free energy behavior (Table 1), which is due to stronger hydrogen bonding and more unfavorable hydrophobic solvation. Because in the peptide the backbone is less solvent accessible than acetamide, it is difficult to make a quantitative estimation of its contribution to $\langle W \rangle$ of the peptide. We will come back to this later.

At the minimum of the PMF most of the peptide is in contact with water, only the hydrophobic side chains of valine are completely desolvated. For a very short peptide, such as a dipeptide, hydrophobic side chains are always solvent exposed in bulk water. Longer peptides might be able to partially shield hydrophobic groups by forming intramolecular hydrophobic contacts. This can be quantified by determining hydrophobic

TABLE 3: Thermodynamics of Transferring Propane from Bulk to Vacuum and Valine Side Chains in Peptides from Bulk to the Air−Water Interface[a]

	molecule	$-\Delta G_{solv}$ (kJ/mol)	V_{bulk} (kJ/mol)	$V_{interface}$ (kJ/mol)	SAS_{bulk} (nm^2)	γ_{prop} (mJ/m^2)	$-\Delta G^*_{Val}$ (kJ/mol)
SPC	propane	-7.8 ± 0.2	-29.5 ± 0.0		-1.59 ± 0.00	38.9 ± 0.2	
SPC/E	propane	-8.9 ± 0.2	-30.5 ± 0.0		-1.59 ± 0.00	41.2 ± 0.2	
	dipeptide		-21.4 ± 0.2	-8.3 ± 0.1	-1.07 ± 0.00		-11.8 ± 0.4
SPC	tetrapeptide		-41.1 ± 0.1	-13.3 ± 0.1	-1.97 ± 0.02		-18.4 ± 0.4
	hexapeptide		-60.3 ± 0.4	-20.4 ± 0.3	-2.83 ± 0.01		-26.3 ± 0.5
	decapeptide		-96.9 ± 0.9	-32.2 ± 1.3	-4.53 ± 0.05		-41.4 ± 2.8
	dipeptide		-22.6 ± 0.1	-7.3 ± 0.2	-1.07 ± 0.00		-11.3 ± 0.3
SPC/E	tetrapeptide		-41.2 ± 0.2	-13.3 ± 0.2	-1.95 ± 0.02		-20.5 ± 0.5
	hexapeptide		-60.0 ± 0.4	-18.8 ± 0.3	-2.79 ± 0.02		-28.0 ± 0.7

[a] V_{bulk} and $V_{interface}$ are the potential energy for the solute−solvent interactions in bulk and at the interface, respectively.

solvent accessible surface (SAS) areas, which are shown in Table 3 (a probe radius of 0.14 nm was used). In bulk, the hydrophobic surface area increase upon addition of a valine (and an asparagine) is around 1 nm^2. All values are less than the SAS area of 1.6 nm^2 of a propane molecule. The difference is caused by the fact that the side chain is connected to the C_α, and therefore part of the side chain is not solvent accessible. A similar difference is observed in the number of water molecules within the first solvation shell. If we define the first solvation shell as all water molecules that have their oxygen atom within 0.5 nm from any of the propane carbons, we obtain 22.5 for propane and around 17 for the valine side chains of the peptides in bulk water. The amount of screening increases only slightly when the peptide size increases, due to some single atom pair contacts between adjacent valine side chains. This is consistent with the fact that we mainly observe extended conformations in the bulk. The peptide lengths in consideration are too short for the formation of a stable hydrophobic core. Only for the decapeptide is a slight deviation from the linearly increasing trend of SAS areas seen. Investigation of the simulation trajectory did not reveal the presence of a stable hydrophobic core.

When a peptide is transferred to the air−water interface, part of the peptide will no longer be in contact with water. The valine side chains avoid solvation in water and have an average of 5 water molecules within 0.5 nm and 90% of time between 1 and 8 water molecules. Although there is some contact with water, this does not seem to affect the structure and hydrogen bonding of the water at the interface. The orientation of the valine side chains fluctuates slightly over time and now and then the side chains touch several water molecules at the interface. These interactions are probably favorable, since they add attractive Lennard-Jones interactions, while not perturbing the hydrogen bonding of the water.

To rationalize the contribution of the desolvation of the side chains to the free energy, we need to make several assumptions. The first is additivity of the different side chains. Since the conformations are mainly extended, there are very few water molecules that are in contact with more than one valine side chain. Furthermore, the conformations of the peptide in bulk and at the interface are very similar; therefore, the side chains will not lose or gain any significant amount intrapeptide of interactions upon transfer to the interface. With this assumption each side chain can be considered separately and the contributions added. To quantify the free-energy change upon transfer of one side chain to the interface, we can use propane as a reference system, since for propane we know the solvation free energy. There are two types of contributions to the hydration of a hydrophobic solute. One is the ordering of water around the solute, as it cannot make hydrogen bonds with the solute; this term is proportional to the SAS area of the solute, although for small solutes it is proportional to the volume.[29] A second contribution comes from the direct van der Waals interactions (LJ in the force field) between the solute and the solvent, for small solutes this term is not proportional to the SAS area. Therefore, we first have to subtract the solute−solvent interaction energy from ΔG_{solv} to obtain an effective surface tension for the water-propane interface. We determined the water−propane interface area from additional simulations of propane in SPC and SPC/E. The resulting effective surface tension γ_{prop} is given in Table 3. Note that the LJ energy is much larger than ΔG_{solv}. These surface tensions are about two-thirds of those at the air−water interface, but the difference between SPC and SPC/E is much smaller in the case of propane solvation. If we assume that the effective surface tension is proportional to the SAS, we can multiply the SAS in the peptide systems with the surface tension and add the side chain−water LJ energy differences to obtain an estimation for the transfer of the side chains from the interface to the bulk (ΔG^*_{Val}). The values are given in Table 3; note that the error estimate contains all statistical errors, but it does not contain errors due to approximations of additivity and linear dependence of the surface area. Since this term is large and involves two important approximations, there is some uncertainty in the values. But we can safely state that these side chain dehydration contributions are equal in magnitude to $\langle W \rangle$ and form the main driving force for transfer of the peptides to the interface.

Another contribution is conformational freedom. Since at the interface the peptide is to a large extent restrained to a two-dimensional space, there will be a loss of conformational entropy of the peptide. For larger molecules, which have more conformational freedom, the loss of entropy at the interface might be higher. To quantify this, we calculated the Shannon entropy s of the peptides:

$$s(x) = -\sum_{i=1}^{n} p(x_i) \log p(x_i) \tag{4}$$

where $p(x_i)$ is the probability of the ith outcome of x. Shannon entropy can be related to thermodynamic entropy[30] (by multiplying with the Boltzmann constant), and it has been widely used in studies to quantify the entropies of the peptides. The absolute value of the Shannon entropy depends on the number of bins used. But when entropy differences are calculated, this dependency drops out when the same number of bins is used. The conformational degrees of freedom can be split into two

TABLE 4: Dihedral and Orientational Entropy Change in kJ/mol upon Transferring the Peptides from the Bulk to the Interface

	pep.	$T\Delta S_d$	$T\Delta S_{ori}$
SPC	dipeptide	−0.1	−2.8
	tetrapeptide	−0.2	−5.5
	hexapeptide	−0.1	−6.7
	decapeptide		−7.9
SPC/E	dipeptide	−0.0	−3.3
	tetrapeptide	−0.2	−5.5
	hexapeptide	−0.1	−6.7

TABLE 5: All the Calculated Contributions to $\langle W \rangle$ as Well as the Rest Term in kJ/mol

	pep.	$\langle W \rangle$	$-T\Delta S_d$	$T\Delta S_{ori}$	$-\Delta G^*_{Val}$	$^1/_4\langle W_{ace} \rangle$	rest
SPC	dipeptide	−11.0	0.1	2.8	−11.8	−2.9	0.8
	tetrapeptide	−17.4	0.2	5.5	−18.4	−4.9	0.0
	hexapeptide	−23.1	0.1	6.7	−26.3	−6.8	3.2
	decapeptide			7.9	−41.4	−13.0	
SPC/E	dipeptide	−14.1	0.0	3.3	−11.3	−3.7	−0.4
	tetrapeptide	−22.8	0.2	5.5	−20.5	−6.1	−1.9
	hexapeptide	−31.6	0.1	6.7	−28.0	−8.6	−1.8

types: intramolecular and molecular orientation. In principle these two sets of degrees of freedom are coupled, but we expect the coupling to be small, so we can analyze them separately to keep the calculation tractable, with the additional advantage that we get two separate numbers. We determined Shannon entropies for the dihedrals of the di-, tetra-, and hexapeptides using bins of 30° for each dihedral, both in bulk water and at the interface. In Table 4 one can see that the intramolecular degrees of freedom indeed lose entropy, but surprisingly, the amount is negligible. For the orientational entropy we determined the two Euler angles that rotate the peptide out of the interface by least-squares fitting to the reference structure, which has the smallest sum of root-mean-square deviation to all other structures. We determined the Shannon entropy using 326 bins of equal size on a sphere (using 732 bins changes the entropy by less than 0.1 kJ/mol for all systems). In Table 4 one can see that the orientational entropy loss is significant. For longer peptides the length dependence decreases, as one would expect. The entropy loss of 1−3 k_BT means that the peptide still has quite some orientational freedom, but part of this might be because the air−water interface is not a rigid, flat surface, but rather a fluctuating interface.

If we assume that we have now treated the major contributions, we can make a decomposition of the free energy of transferring a peptide from the bulk to the air−water interface. We have made several approximations and neglected several effects, but we should have captured all the major contributions. We can add up the contributions and determine the difference with $\langle W \rangle$. Since the backbone dehydration is too complex to quantify directly, we simply scaled it by a constant to make the total $\langle W \rangle$; this constant turns out to be a quarter. Note that the number of acetamides in this calculation is equal to the numbers of residues plus one, since there are that many peptide bonds. The rest terms (see Table 5) comply with the statistical error of around 2 kJ/mol. However, the rest term is systematically positive for SPC and negative for SPC/E. This indicates that a (small) water model dependent contribution is missing or underestimated. We can look at water model dependence more accurately by determining the $\Delta\Delta G$ for hydration between SPC and SPC/E.

IV. $\Delta\Delta G$ Calculations

The difference in hydration free energy between the two water models, both in bulk water and at the air−water interface, can tell something about the nature of the free-energy differences upon transfer to the interface. Determining a ΔG of hydration of a peptide is a computationally expensive task, especially at the interface where long sampling is required. It turns out to be computationally much cheaper to change SPC water into SPC/E. Using Bennett's acceptance ratio method,[31,32] this can done in 10 ns with just one intermediate state for water and the dipeptide system. The error was estimated by block averaging using 5 blocks of 2 ns. The result is a $\Delta\Delta G$ of 3.3 ± 0.3 kJ/mol for bulk water and a $\Delta\Delta G$ of −0.3 ± 0.3 kJ/mol at the interface. The difference between these numbers nicely matches the $\Delta\langle W \rangle$ obtained from the PMF calculations in SPC and SPC/E. For the hexapeptide we only performed the calculation in bulk water, with three intermediate states; the result is 14.3 ± 1.2 kJ/mol. The difference between SPC and SPC/E matches the sum of the difference of the hydration free energies of the components listed in Table 1, assuming that the backbone matches acetamide and the difference for the terminal methyl groups is negligible. For the dipeptide the difference vanishes at the interface. The dipeptide $\Delta\Delta G$ between bulk and interface, between SPC and SPC/E is −3.6 kJ/mol. This is 2−3 times as much as our free energy decomposition gave with the hydration free energy difference of propane plus $3/4\Delta\langle W \rangle$ of acetamide. This again shows there is a slightly larger water model dependence than our analysis provides, probably due to an oversimplified analysis of the backbone contribution and ignoring the effect of the termini.

V. Surface Tension

Reduction of the surface tension is also a key element in driving the peptides to the air−water interface. To determine the surface tension reduction when the interface is covered with peptides, we solvated 40 randomly placed tetrapeptides in an interface of 2000 SPC/E water molecules. Using a cubic initial volume turned out to produce quite stable clusters of peptides in the bulk in addition to peptides at the interface. Therefore, we started with a slab of 6 × 6 × 2.5 nm, which we slowly deformed to a slab of 3.8 × 3.8 × 6 nm. The final state has 19 peptides on the top and 21 peptides on the bottom interface, where a representative snapshot from the top surface is shown in Figure 5. After equilibration the surface density of the peptides is around 1.2 peptides per nm^2.

The dehydration of valine side chains, which provides the largest contribution to the transfer free energy, does not contribute significantly to the surface tension reduction. Although a lot of free energy is gained by moving these side chains out of bulk water, valine side chains are too small to cover the surface completely. In fact, valine side chains remain completely isolated from the rest of the system. On the other hand, the peptide backbones shield water molecules by forming a continuous layer connected via hydrogen bonds.

The surface tension is difficult to estimate accurately, since fluctuations are larger and convergence is slower compared to the case of pure water. If we ignore the first 100 ns as equilibration, we obtain 41 ± 2 mJ/m^2 for the final 100 ns. This is a reduction of the surface tension by 30%, or a reduction of 9 ± 2 kJ/mol per peptide. Note that the free-energy difference between peptides dispersed in bulk and a layer of peptides at the interface involves not only the free energy difference of transfer of a single peptide from bulk to the interface but also

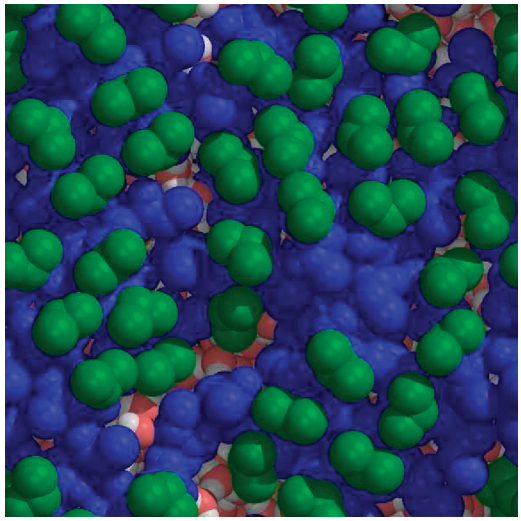

Figure 5. Top view of 19 tetrapeptides (in blue) at the air−water interface. Note that the valine side chains (in green) are nearly all separated from the rest of the system.

the favorable free energy contributions of the interactions between two or more peptides at the interface.

VI. Conclusions

We have accurately determined the free energy of transferring peptides from bulk water to the air−water interface, for the given force field and two water models. The $\Delta\Delta G$ between the two water models has been verified with free energy transformations using Bennett's acceptance ratio. The minimum of the PMF is deep: between 5 and 11 k_BT. Absolute free energy values cannot be given, since there is an entropic term in the free energy that depends on the height of the bulk water phase below the interface. The shape of the PMF is the same for all peptides and water models with one deep minimum with a (thermal) width of a few Ångstroms. We have shown that the ΔG of amphiphilic peptides is dominated by one favorable contribution: the desolvation of hydrophobic side chains. For these peptide lengths two smaller terms are the partial dehydration of the backbone and the loss of orientational entropy, which is the only significant unfavorable term. In SPC/E ΔG is 30% larger than in SPC. This difference is caused by the stronger hydrophobic effects in SPC/E, which appear in the dehydration of both the backbone and the valine side chains. This means that for quantitative modeling the choice of water model is critical. SPC/E is a better choice than SPC, since it reproduces hydrophobic hydration thermodynamics much better than SPC. This is also reflected in the surface tension of the water models. However, SPC/E still underestimates the surface tension by 15%. It remains to be seen what effect this discrepancy has on the partitioning of amphiphilic molecules to the interface.

There are also contributions that disfavor the transfer of a peptide to the air−water interface. The largest one is the restriction of the orientation of the peptide at the interface. This term is 1 k_BT for the dipeptide up to 3 k_BT for the decapeptide. We also expected some entropy loss of the internal degrees of freedom of the peptide, but this does not seem to be the case. The net effect of the three main contributions produces a free energy difference that is linear for the chosen sequence at least up to hexapeptides, but probably also up to decapeptides. At a certain length this linear increase will level off, since in bulk a long peptide will be able to form contacts between hydrophobic side chains in bulk water, thereby shielding hydrophobic groups from the solvent. For the decapeptide we see this happening to a minor extent. An effect that might play a role in experiments, but that is beyond the scope of this work, is the clustering of peptides in bulk water. At high concentrations peptides will come together to shield off hydrophobic groups from the solvent. At the interface the peptides cluster through intramolecular hydrogen bonds between backbones. The resulting layer lowers the surface tension by 30% compared to the surface tension of a pure SPC/E air−water interface.

The three main contributions to the free energy difference depend strongly as well as differently on the length and the composition of the molecule; therefore, it is difficult to predict the partitioning behavior of general peptide sequences at the air−water interface. The behavior of complete proteins at the interface varies widely with sequence (see, e.g., ref 33). However, we have shown that the thermodynamics for peptides with alternating hydrophobic/hydrophilic sequences is relatively simple. The driving force is the reduction of hydrophobic interface area with water, for both hydrophobic side chains and the hydrophobic air interface. The only significant opposing force is the loss of orientational entropy of the peptide at the interface, but this term is relatively small. Therefore, alternating hydrophobic/hydrophilic sequences will partition strongly to a hydrophobic/hydrophilic interface, without frustration.

Acknowledgment. M.S. and O.E. thank TUBITAK (106T575) and the Max Planck Society for financial support through the Partner Group Agreement with Prof. Kurt Kremer's Theory Group at MPIP, Mainz. We also thank Dr. Raymond Tu and his group for scientific discussions and sharing their experimental results on the peptide molecule. B.H. thanks Dr. Sander Pronk for extensive discussions on surface tension effects.

Appendix A: Center of Mass in a Periodic System

In umbrella sampling one often needs a potential that acts on the centers of mass (COM) of groups of particles. Without periodic boundary conditions or for spatially confined groups this is not an issue; one can simply use the mass-weighted averaged coordinates of the particles in the group. But when a group consists of several molecules in a periodic system, problems will occur when a molecule moves one periodic distance with respect to the other molecules in the group. We will derive a general solution to this problem.

Consider a group of N particles with coordinates x_i and masses m_i. These particles are part of a larger system, the size of which is irrelevant for this derivation. For umbrella sampling one would like to add a potential $V_u(X)$ or $V_u(X_1,X_2)$ that acts on the COM X or the distance between COMs. The following derivation will be one-dimensional, extension to multiple dimensions is trivial.

We will define $X(\boldsymbol{x})$ as the coordinate that minimizes the mass weighted sum of a spatial function s as follows:

$$\min_X \sum_{i=1}^{N} m_i\, s(x_i - X) \tag{5}$$

To minimize this, one needs to solve

$$\sum_{i=1}^{N} m_i\, s'(x_i - X) = 0 \tag{6}$$

for X and check the sign of the second derivative. The force due to the umbrella on particle i is

$$f_i = -\frac{\mathrm{d}V_u(X(\mathbf{x}))}{\mathrm{d}x_i} = -\frac{\mathrm{d}V_u(X)}{\mathrm{d}X}\frac{\mathrm{d}X(\boldsymbol{x})}{\mathrm{d}x_i} \tag{7}$$

To evaluate f_i, we need the derivative of X with respect to x_i. We can obtain this through a first-order expansion of eq 6 around $x_i - X$. The zeroth-order term is zero by definition, so we are left with

$$m_i s''(x_i - X)\,\mathrm{d}x_i - \sum_{j=1}^{N} m_j\, s''(x_j - X)\,\mathrm{d}X = 0 \tag{8}$$

The derivative is then

$$\frac{\mathrm{d}X}{\mathrm{d}x_i} = \frac{m_i\, s''(x_i - X)}{\sum_{j=1}^{N} m_j\, s''(x_j - X)} = \frac{m_i w_i}{\sum_{j=1}^{N} m_j w_j} \tag{9}$$

where we have introduced w_i, the weight of particle i.

For $s(x) = x^2$ we recover the standard COM. Equation 6 can be solved directly, since s' is linear and the weights given by eq 9 are proportional to the masses since s'' is constant. In this framework it is obvious that the standard COM will fail in periodic systems, since x^2 is not a periodic function. The solution is straightforward: use a periodic function for s. The simplest choice is

$$s(x) = \cos\left(\frac{2\pi x}{l}\right) \tag{10}$$

where l is the length of the periodic unit cell. Equation 6 can be solved directly:

$$X = \frac{l}{2\pi}\arctan\left(\frac{\sum_{i=1}^{N} m_i \sin(2\pi x_i/l)}{\sum_{i=1}^{N} m_i \cos(2\pi x_i/l)}\right) \tag{11}$$

This choice of s will produce a unique X for all coordinate distributions, except those that are periodic with a period of half the box length. For the particular case of a slab of particles in contact with a vapor, the relative weights of particles at the edges of the slab will be smaller than in the middle. For a slab thickness of a quarter of the unit cell the difference is weights is up to $^1/_2\sqrt{2}$, while for a thickness of a third of the unit cell it is $^1/_2$. In most cases this weight difference will not have a significant effect, since the force on the COM is distributed over a large number of particles. When a particle escapes from the slab and travels through the unit cell, its weight will decrease and might become negative, meaning that the force on the escaped particle will have the opposite direction compared to the other particles. The particle can merge back into the slab having crossed through the periodic boundary without causing jumps in the potential or the force as would occur with a standard COM.

Instead of adding an umbrella potential on a COM, another option is constraining a COM. Constraints can be added to the Hamiltonian with the principle of least action through a Lagrange multiplier. We will not go into the details of the procedure here and only provide the solution. What is required additionally for a constraint is the effective mass of the COM, this is

$$m_X = \frac{(\sum_{i=1}^{N} m_i w_i)^2}{\sum_{i=1}^{N} m_i w_i^2} \tag{12}$$

The COM constraint can then be solved as a normal constraint. What remains to be done is redistribute the constraint displacement ΔX to the particles. This is done proportional to the weights as follows:

$$\Delta x_i = \frac{\sum_{j=1}^{N} m_j w_j w_i}{\sum_{j=1}^{N} m_j w_j^2}\Delta X \tag{13}$$

It can be verified easily that the sum of the mass times displacement of the particles equals $m_X \Delta X$.

For constraining a COM with $s(x) = \cos(x)$, seven sums are required involving masses, cosines, and sines, five for the reference coordinates, and two for the unconstrained coordinates. These seven sums can be accumulated in a single loop and, with parallel simulation, can be summed at once over all the processors. The main additional cost compared to that for a standard COM calculation is the evaluation of one cosine and sine per particle, which is negligible in most cases.

References and Notes

(1) Kuzmenko, I.; Rapaport, H.; Kjaer, K.; Als-Nielsen, J.; Weissbuch, I.; Lahav, M.; Leiserowitz, L. *Chem. Rev.* **2001**, *101*, 1659.

(2) Fan, H.; Wang, X.; Zhu, J.; Robillard, G. T.; Mark, A. E. *Proteins: Struct. Funct. Genet.* **2006**, *64*, 863.

(3) Miller, C. A.; Abbott, N. L.; de Pablo, J. J. *Langmuir* **2009**, *25*, 2811.

(4) Maget-Dana, R. *Biochim. Biophys. Acta* **1999**, *1462*, 109.

(5) Krejchi, M. T.; Atkins, E. D. T.; Waddon, A. J.; Fournier, M. J.; Mason, T. L.; Tirrell, D. A. *Science* **1994**, *265*, 1427.

(6) Rapaport, H. *Supramol. Chem.* **2006**, *18*, 445.

(7) Zasloff, M. *Nature* **2002**, *415*, 389.

(8) Maget-Dana, R.; Lelievre, D.; Brack, A. *Biopolymers* **1999**, *49*, 415.

(9) Powers, E. T.; Yang, S. I.; Lieber, C. M.; Kelly, J. W. *Angew. Chem.* **2002**, *41*, 127.

(10) Volinsky, R.; Kolusheva, S.; Berman, A.; Jelinek, R. *Langmuir* **2004**, *20*, 11084.

(11) Garrett, B. C.; Schenter, G. K.; Morita, A. *Chem. Rev.* **2006**, *106*, 1355.

(12) Gu, C.; Lustig, S.; Jackson, C.; Trout, B. L. *J. Phys. Chem. B* **2008**, *112*, 2970.

(13) Oostenbrink, C.; Villa, A.; Mark, A. E.; van Gunsteren, W. F. *J. Comput. Chem.* **2004**, *25*, 1656.

(14) Berendsen, H. J. C.; Postma, J. P. M.; van Gunsteren, W. F.; Hermans, J. In *Intermolecular Forces*; Pullman, B., Ed.; D. Reidel Publishing Co.: Dordrecht, The Netherlands, 1981; pp 331−342.

(15) Berendsen, H. J. C.; Grigera, J. R.; Straatsma, T. P. *J. Phys. Chem.* **1987**, *91*, 6269.

(16) Hess, B.; van der Vegt, N. F. A. *J. Phys. Chem. B* **2006**, *110*, 17616.

(17) Wolfenden, R.; Andersson, L.; Cullis, P. M.; Southgate, C. C. B. *Biochemistry* **1981**, *20*, 849.

(18) Makhatadze, G. I.; Privalov, P. L. *J. Mol. Biol.* **1993**, *22*, 639.

(19) Hess, B.; Kutzner, C.; van der Spoel, D.; Lindahl, E. *J. Chem. Theory Comput.* **2008**, *4*, 435.

(20) Essmann, U.; Perera, L.; Berkowitz, M. L.; Darden, T.; Lee, H.; Pedersen, L. G. *J. Chem. Phys.* **1995**, *103*, 8577.

(21) Berendsen, H. J. C.; Postma, J. P. M.; van Gunsteren, W. F.; Di Nola, A.; Haak, J. R. *J. Chem. Phys.* **1984**, *81*, 3684.

(22) Miyamoto, S.; Kollman, P. A. *J. Comput. Chem.* **1992**, *13*, 952.

(23) Hess, B. *J. Chem. Theory Comput.* **2008**, *4*, 116.

(24) In-Chul, Y.; Berkowitz, M. L. *J. Chem. Phys.* **1999**, *111*, 3155.

(25) Hess, B. *J. Chem. Phys.* **2002**, *116*, 209.

(26) MacRitchie, F. *Chemistry at Interfaces*; Academic Press: New York, 1990.

(27) In 't Veld, P. J.; Ismail, A. E.; Grest, G. S. *J. Chem. Phys.* **2007**, *127*, 144711.

(28) Bussi, G.; Donadio, D.; Parrinello, M. *J. Chem. Phys.* **2007**, *126*, 014101.

(29) Huang, D. M.; Geissler, P. L.; Chandler, D. *J. Phys. Chem. B* **2001**, *105* (28), 6704.

(30) Jaynes, E. T. *Phys. Rev.* **1957**, *106* (4), 620.

(31) Bennett, C. H. *J. Comput. Phys.* **1976**, *22* (2), 245.

(32) Shirts, M. R.; Bair, E.; Hooker, G.; Pande, V. S. *Phys. Rev. Lett.* **2003**, *91* (14), 140601.

(33) Martin, A. H.; Cohen Stuart, M. A.; Bos, M. A.; van Vliet, T. *Langmuir* **2005**, *21*, 4083.

JP1024922